

BACHELOR

Analysis of a vibration isolated test bench

de Groot, G. (Bert)

Award date:
2023

[Link to publication](#)

Disclaimer

This document contains a student thesis (bachelor's or master's), as authored by a student at Eindhoven University of Technology. Student theses are made available in the TU/e repository upon obtaining the required degree. The grade received is not published on the document as presented in the repository. The required complexity or quality of research of student theses may vary by program, and the required minimum study period may vary in duration.

General rights

Copyright and moral rights for the publications made accessible in the public portal are retained by the authors and/or other copyright owners and it is a condition of accessing publications that users recognise and abide by the legal requirements associated with these rights.

- Users may download and print one copy of any publication from the public portal for the purpose of private study or research.
- You may not further distribute the material or use it for any profit-making activity or commercial gain

Department of Mechanical Engineering

De Rondon 70, 5612 AP Eindhoven P.O.
Box 513, 5600 MB Eindhoven
The Netherlands
www.tue.nl

Author
Bert de Groot (1459597)

Responsible Lecturer
Rob Fey

Date
February 12, 2023

Analysis of a vibration isolated test bench

Bachelor End Project

Bert de Groot (1459597)
g.d.groot@student.tue.nl

Table of contents

Title		
Analysis of a vibration isolated test bench	1 Introduction	1
	2 List of symbols	2
	3 Construction elaboration	3
	3.1 Base assembly	4
	3.2 Table top assembly	5
	3.3 Connection	6
	4 Requirements	8
	4.1 Problem description	8
	4.2 Value conversions	8
	4.3 Reaction forces	10
	4.4 Constraints in frequency domain	11
	5 Analytical modelling	13
	5.1 Assumptions	13
	5.1.1 X direction	13
	5.1.2 Z direction	13
	5.2 Analytical approach	14
	5.2.1 X direction	14
	5.2.2 Z direction	15
	5.3 Lumped mass model	17
	5.3.1 Masses	17
	5.3.2 Transfer functions	18
	6 Measurements	20
	6.1 Instrument selection	20
	6.2 Test plan	20
	6.3 Measurements	21
	6.3.1 X direction	21
	6.3.2 Additional measurement	22

Table of contents

Title		
Analysis of a vibration isolated test bench	6.3.3 Z direction	22
	6.4 Analysis	23
	6.4.1 X direction	23
	6.4.2 Z direction	24
	7 Conclusion	25
	8 Recommendations	26
	8.1 Recommendations for future research	26
	8.2 Foundings on the current setup	26
	Appendix A Appendix A	27
	A.1 Constraints	27
	A.2 Analytical approach	28
	A.3 Measurements	29
	Appendix B Appendix B	42
	B.1 Analytical solution	42
	B.1.1 α Values	42
	B.1.2 Derivation of the transfer function with floor disturbance as input	42
	B.1.3 Derivation of the transfer function with reaction forces as input	43
	B.1.4 Deformation top beams	43
	B.2 Measurements	43

1 Introduction

Prodrive-technologies produces a microscope that operates with three servo actuated moving stages. Functional tests on this product tend to fail to frequent. It is expected that the assembly table on which the test is performed is the main cause of this. The reason for this is that the table most likely cannot handle the floor vibrations, the reaction forces of the stages or a combination of both. The goal of this report is to analyse how the table reacts to floor vibrations and reaction forces for different frequencies. This will be done by determining the important stiffnesses of the table analytically and by measurements. After that the frequency response will be plotted showing how the table reacts to inputs.

In chapter 3 of this report, an elaboration on the assembly table is given to clarify the design. In chapter 4, the allowed errors for each stage given by Prodrive-technologies are converted to errors at a more useful location and from time domain to the frequency domain. The reaction forces from the stages are also computed in frequency domain. Chapter 5 is dedicated to the analytical approach of the setup, the stiffness are analytically determined and the transfer functions are created. In chapter 6, a test plan is stated together with the resulting stiffnesses. These results are then plotted into a bode plot and analysed. This report only considers the X and Z direction of the microscope due to time constraints.

2 List of symbols

Symbol	Variable	Unit	Abbreviation
a	Acceleration	Meter per second squared	ms^2
b	Distance	Meter	m
d	Damping coefficient	Newton second per meter	Nsm^{-1}
E	Youngs' Modulus	Giga Pascal	GPa
f_{bw}	Bandwidth frequency	Hertz	Hz
I	Area moment of inertia	Meters to the power of four	m^4
J	Jerk	Meter per second cube	ms^{-3}
K_p	Proportional gain	-	-
K_{fa}	Feedforward acceleration constant	Ampere seconds squared per meter	As^2m^{-1}
K_{fv}	Feedforward velocity constant	Ampere second per meter	Asm^{-1}
L,l	Length	Meter	m
m	Mass	Kilogram	kg
p	Position	Meter	m
t	Thickness	Meter	m
v	Velocity	Meter per second	ms^{-1}
X	Position	Meter	m
ζ	Damping ratio	-	-
ω_{bw}	Angular velocity	radians per second	$rad s^{-1}$

3 Construction elaboration

The current assembly table on which the test is performed is shown in Figure 3.1. The table consists of a base assembly and a table top assembly, which are able to slide relative to each other. They are shown separately in Figure 3.2a and Figure 3.2b. Both assemblies are made of aluminum extrusion profiles. Note that the X and Y direction of the CAD drawings are not the same directions as with the stages. The X stage of the microscope is pointed in the Y direction of the CAD model.

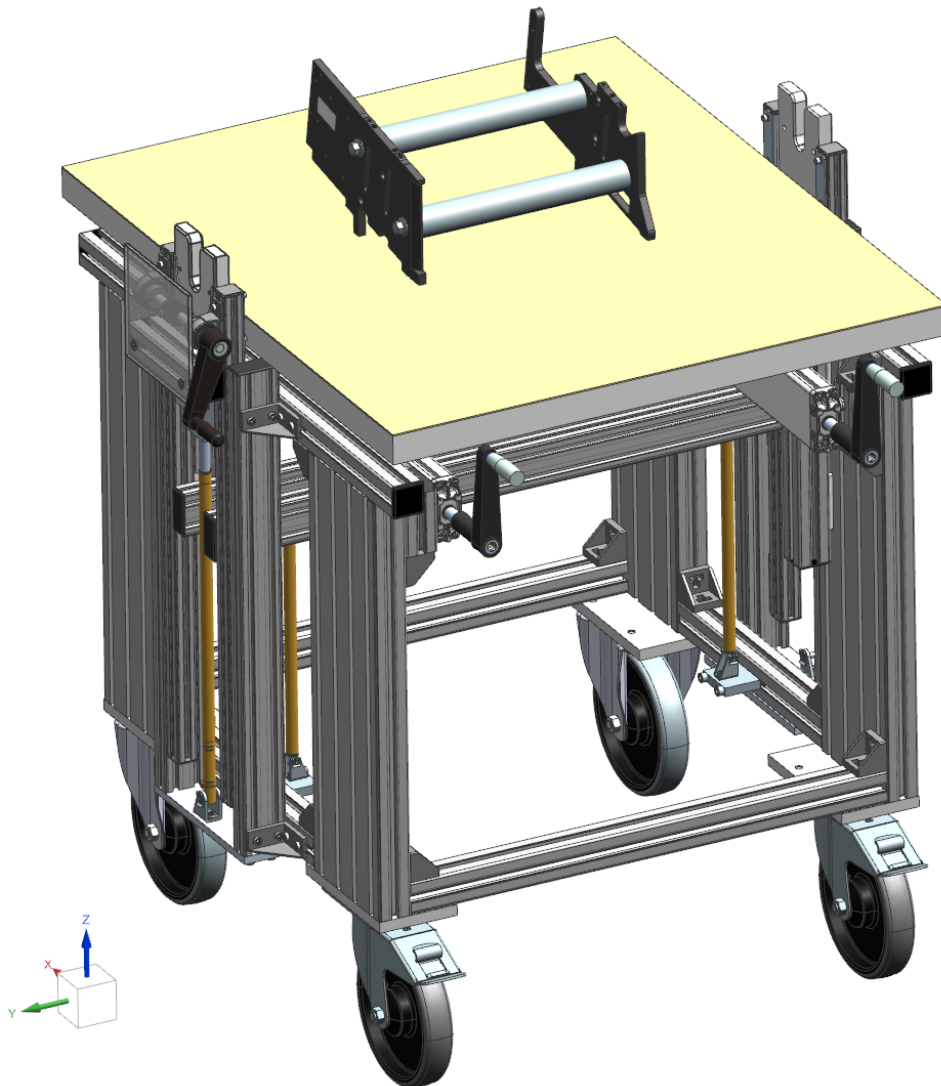


Figure 3.1: Table setup

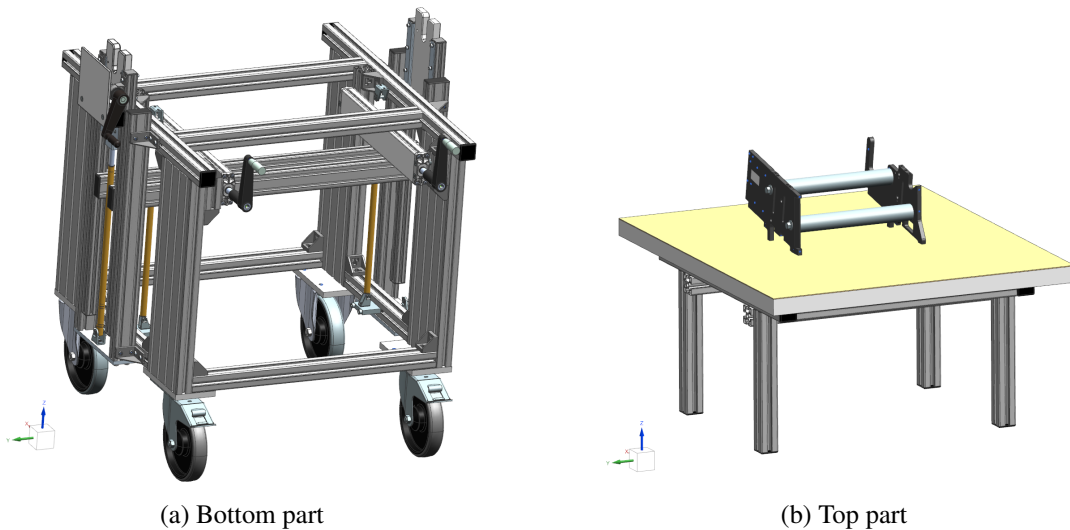


Figure 3.2: Top and bottom part of the table shown separately

3.1 Base assembly

The base assembly is described from the bottom upwards. It starts with four wheels, two of which are swivel caster wheels (CW), the other two are fixed caster wheels (FW). On top of these wheels, a cuboid-shaped frame is placed, a more clear figure of this sketch is given in Figure 3.3a. The vertical beams of this frame (main beams) have a cross section around four times as large as the other beams. The two horizontal beams on top of the frame are labelled as the 'top beams'. The way this frame is mounted onto the wheels is clarified in Figure 3.3b. As can be seen, the wheels are mounted to a thick, solid aluminum plate. Two bolts are then connecting the plate with the main beams, which has threaded holes in it. The two horizontal beams visible in Figure 3.3b are connected to the main beam with angle brackets.

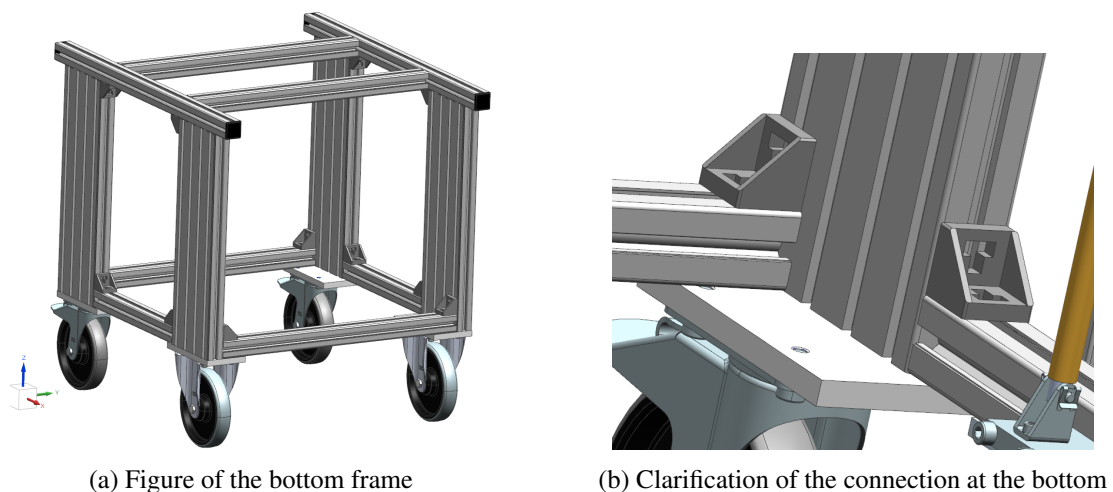


Figure 3.3: Overview of the square frame and its connection at the bottom

The base assembly has a special function implemented into it, it has a lifting mechanism attached on the side. This mechanism is used to lift the microscope from the table and rotate it to make assembly easier. This mechanism is attached to the frame with two vertical beams (outer beams) on each side. The connection of these beams is annotated in Figure 3.4a, a clear figure of which parts of the lifting mechanism can move is given in Figure 3.4b.

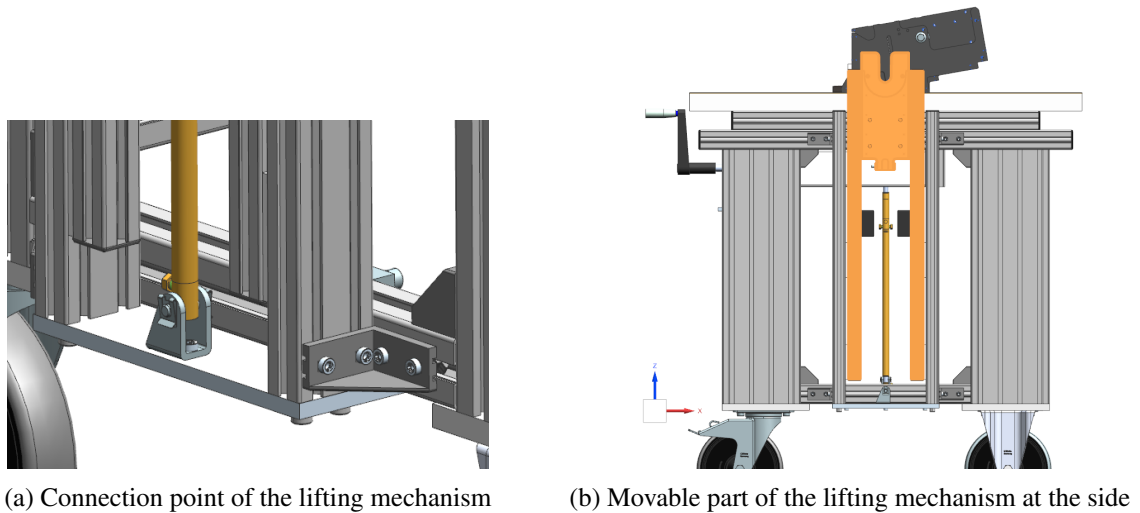


Figure 3.4: Overview of the lifting mechanism at the side and its connection at the bottom

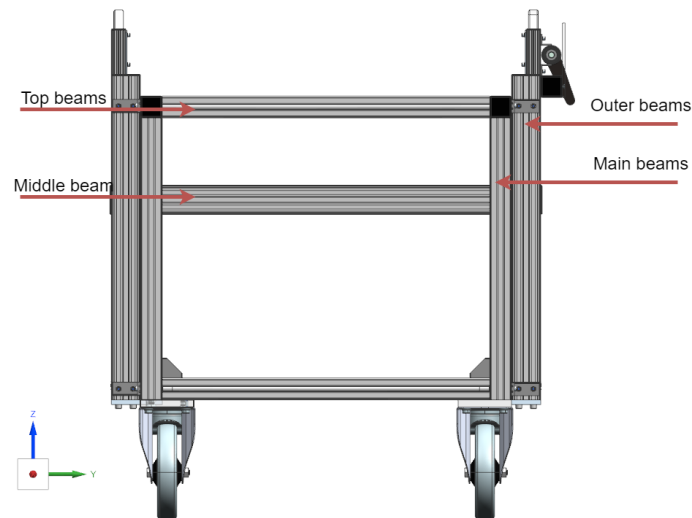


Figure 3.5: Beam labels on the bottom part

3.2 Table top assembly

The top part has a tabletop made of chipboard. Underneath this tabletop, an aluminum frame is mounted. This frame is visualized in Figure 3.6 together with the labels for the beams. This frame has then four vertical beams pointing downwards, these beams are used as linear guiding when the top part is being moved up. The actuation of this lifting mechanism is through the hydraulic system mounted on the frame assembly.

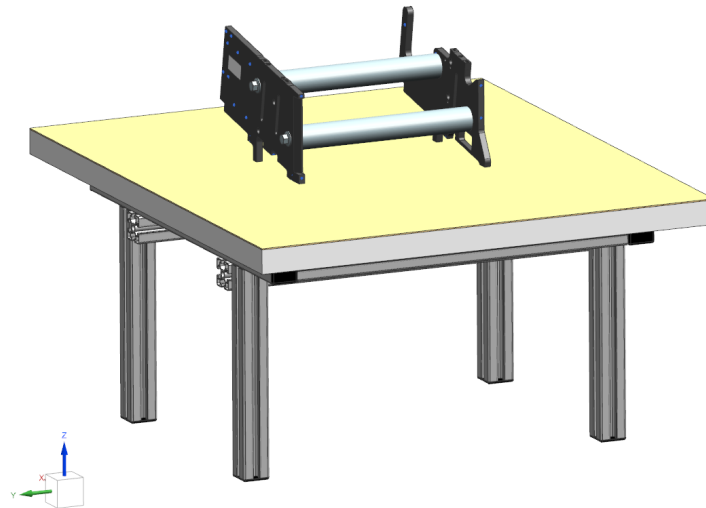
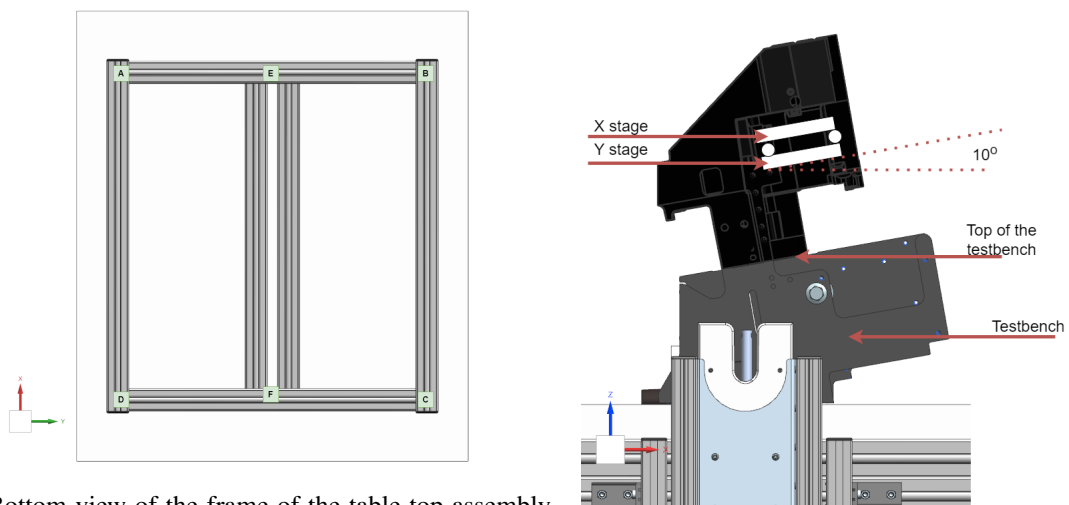


Figure 3.6: Overview of the table top assembly

On top of the tabletop, the testbench is placed, it is not fixed to the tabletop. This testbench consists of two custom made aluminum plates with two shafts to connect the plates. The function of this testbench is to represent the stiffness which would be provided by the frame of the microscope once the product is finished. The microscope is then placed on top of this testbench, this spot is labeled as top of the testbench.



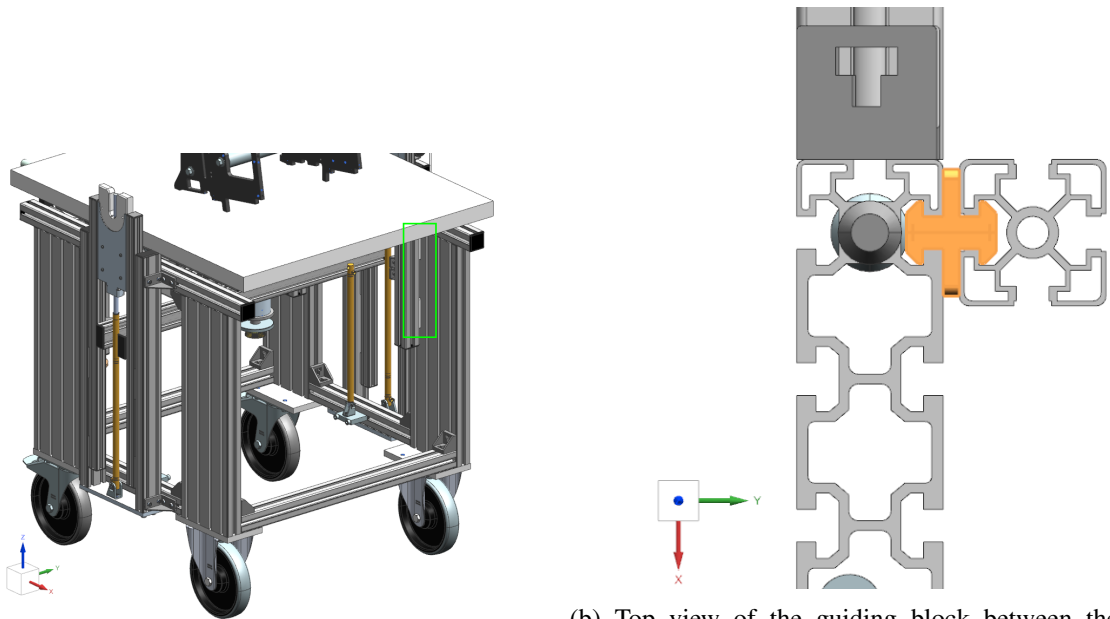
(a) Bottom view of the frame of the table top assembly with labels

(b) Labels of the testbench and orientation of the stages

Figure 3.7: Labels used for the top part

3.3 Connection

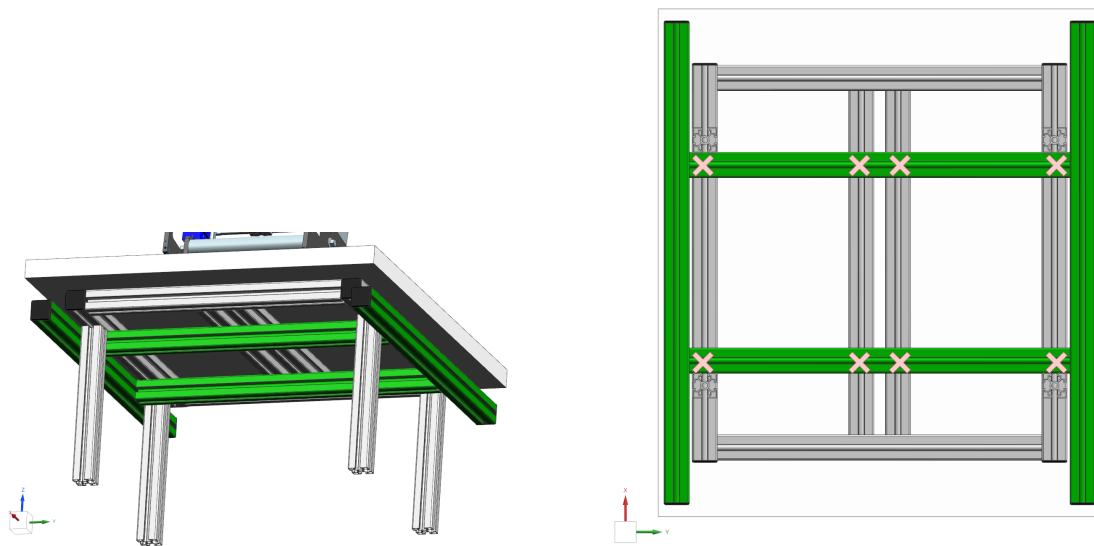
The top part is placed on top of the lower part, they are connected through linear guiding blocks. Every corner has two of these guiding blocks, so a total of 8 blocks are present. The locations and a top view of this guiding block is shown in Figure 3.8. Next to that, on both sides of the table, a piston is placed to control the height of the tabletop.



(a) Location of one of the guiding blocks in the design beams, the guiding block is marked orange
 (b) Top view of the guiding block between the two

Figure 3.8: Clarification on the guiding block between the bottom and top part

During tests, the top part is lowered to its lowest position, therefore the lifting mechanism will not be of much importance for this project. In the lowest position, the top part rests on the frame of the bottom part. The contact points of the two parts is visualized in Figure 3.9b. Due to the mass of the top part and the frame of the microscope combined, the friction force will be big enough to prevent the top and bottom part from shifting relative to each other horizontally during tests.



(a) Connection bottom and top part where the bottom part is marked green
 (b) Connection points between the top and bottom part marked

Figure 3.9: Connection between the top and bottom part

4 Requirements

4.1 Problem description

The main problem with the current setup is that due to both disturbances coming from the floor and disturbances due to reaction forces of the stage itself, the location where the microscope is placed is vibrating. This causes tests, which verify the accuracy of the microscope, to fail and is therefore not desired.

The table below has been provided by Prodrive-Technologies as part of the problem description. It gives the main requirements on the allowed error of all three stages. The maximum allowed error is given at the encoders of each of the stages. For this project, it is more useful to have the maximum error at the top of the test bench as the microscope itself cannot be changed, but changes can only be made to the table assembly. The defined location of the test bench at which the maximum allowed error is, is shown in Figure 3.7. As the actuators of the microscope have feedback controllers, these actuators are able to partially correct the error. To get these requirement values, the given errors need to be converted into the allowed error at the testbench, this is done in section 4.2. The table also provides information about the vibrations due to the oscillating of the floor, a clear graph of how this looks like is given in Figure A.4.

Table 4.1: Requirements and information about the stages and the floor disturbances given by Prodrive-technologies

Property	Value	Unit	Remark
Moving mass stage X	5	kg	
Moving mass stage Y	2	kg	Axis provided with brake
Moving mass stage Z	0.5	kg	
Base frame mass	20	kg	
Max. allowed velocity error X	0.25	mm/s	Due to floor and test bench vibrations
Max. allowed position error Y	25	nm	After settling, due to floor and test bench vibrations
Max. allowed position error Z	50	nm	Due to floor and test bench vibrations
Floor vibrations, 4 - 8 Hz	800 - 400	$\mu\text{m/s}$	ISO, office level
Floor vibrations, 8 - 80 Hz	400	$\mu\text{m/s}$	ISO, office level

4.2 Value conversions

The position of the stages are controlled by PID controllers with a closed loop. This closed loop will help to correct for external disturbances. The maximum error at the top of the test bench is desired, the maximum relative error between the frame of the microscope and the frame is given. When the maximum error is converted to the maximum error at the top of the testbench, this closed loop should be taken into account.

To take the closed loop into account, the force exerted by the actuator is assumed to be a spring. This assumption can be made as the highest disturbance frequency is at 4Hz. The PID controller can be assumed to only have a proportional part if the frequency of the disturbance is significantly lower than the bandwidth. This is the case for the input frequency of 4Hz as the bandwidths of the three stages are between 60Hz and 150Hz.

A proportional controller can be considered as a spring with a spring coefficient. In order to know the force exerted by this controller, the spring coefficient is required. This value is obtained in the following formula and its rewritten form

$$\omega_{bw} = \sqrt{\frac{K_p}{m}} = 2 \cdot \pi \cdot f_{bw} \quad (4.1)$$

$$K_p = (2 \cdot \pi \cdot f_{bw})^2 \cdot m \tag{4.2}$$

Where ω_{bw} is the angular frequency at the bandwidth, K_p is the spring coefficient, m is the moving mass and f_{bw} is the bandwidth frequency.

With this spring coefficient known, the force and with that the acceleration and velocity of the actuator can be computed. For the required reaction force to keep the stages at the correct location, the actuator is taken as a closed loop where the output force is equal to the proportional part of the controller multiplied by the error. A schematic of this can be seen in Figure 4.1.

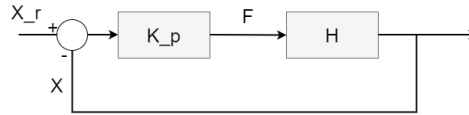


Figure 4.1: Representation of the closed loop system used to determine the maximum force the stage can handle without failing on tests

Now the following formulas can be applied in order to get the force corresponding to the allowed error of the stage. Equation 4.3 converts the error to the force by approaching it as a spring. After that, the acceleration is obtained, with that acceleration the maximum allowed disturbance velocity is obtained. This value is the requirement that is applicable at the top of the test bench. Velocity can be obtained by integrating the acceleration over time. The time in this case is equal to the frequency multiplied by $2 \cdot \pi$. The frequency is equal to the disturbance frequency. For the disturbance frequency, the lowest frequency of the frequency range has been picked, 4 Hz, as this gives the highest disturbance velocities.

$$F = K_p \cdot (X - X_r) = K_p \cdot e \tag{4.3}$$

$$a = \frac{F}{m} \tag{4.4}$$

$$v = \frac{a}{2 \cdot \pi \cdot f_{dist}} \tag{4.5}$$

The input values for the above formulas and the results obtained from the equations can be found in the table below

Table 4.2: Values used to compute the allowed error at the testbench together with the allowed error

	X	Y	Z
f_bw	80Hz	60Hz	150Hz
e	0.25mm/s	25nm	50nm
m	5kg	2kg	0.5kg
f_dist	4Hz	4Hz	4Hz
resulting error	5mm/s	1.414mm/s	1.8mm/s

As the error of the X direction was given in [mm/s] while the Y and Z directions error was given in [nm], this velocity error is converted as well. This was done as shown below by using the bandwidth frequency, the used formula is shown below.

$$e_v = \frac{e_p}{2 \cdot \pi \cdot f_{bw}} \tag{4.6}$$

Where e_v is the velocity error and e_p the position error.

4.3 Reaction forces

In order to determine the reaction forces from the microscope onto the test setup, the acceleration is required. To get this acceleration, a motion profile is made[3]. The following values have been used as inputs. The motion profile for X, Y and Z direction have been made. This is due to the fact that the Y stage is located under a 10° angle, it has therefore a force in Z direction as well, this force in the Z direction due to the reaction force of the Y direction is what will be computed.

Table 4.3: Values used to determine the motion profile

		Value	Unit
X direction	$J_{max,X}$	150	$\frac{m}{s^3}$
	$a_{max,X}$	1	$\frac{m}{s^2}$
	$v_{max,X}$	8e-3	$\frac{m}{s}$
	p_X	0.0342	m
	m_x	5	kg
Y direction	$J_{max,X}$	150	$\frac{m}{s^3}$
	$a_{max,X}$	1	$\frac{m}{s^2}$
	$v_{max,X}$	50e-3	$\frac{m}{s}$
	p_X	0.1251	m
	m_x	5	kg
Z direction	$J_{max,Z}$	150	$\frac{m}{s^3}$
	$a_{max,Z}$	0.5	$\frac{m}{s^2}$
	$v_{max,Z}$	5e-3	$\frac{m}{s}$
	p_Z	0.00295	m
	m_Z	0.5	kg

With J_{max} being the maximum Jerk on the system, a_{max} the maximum acceleration, v_{max} the maximum velocity and p the maximum distance the stage could travel. M represents the moving mass of the corresponding directions stage. The resulting motion profiles can be found in section A.1.

The force can now be determined from the acceleration of the motion profile. This is done with the following equation.

$$F = m \cdot a + \frac{m \cdot K_{fv}}{K_{fa}} \cdot v \quad (4.7)$$

where F is the reaction force, a the acceleration obtained from the motion profile, m the moving mass of the stage, K_{fv} the feedforward velocity constant, K_{fa} the feedforward acceleration constant and v the velocity of the stage obtained from the motion profile.

This force can be plotted in the frequency domain with a Fast Fourier Transform function (FFT). The frequency response functions (FRF), where force is plotted against frequency, for both X and Y direction are shown in Figure 4.3. It can be seen that the FRF for both X and Y direction is constant and at one point, goes down linearly with both axis having a logarithmic scale. Therefore, the maximum force can be linearized by drawing a line following the maximum force values. This linear representation is easier to work with compared to the actual FRF and it represents the most important values from the graphs as it shows the maximum force of the system per frequency.

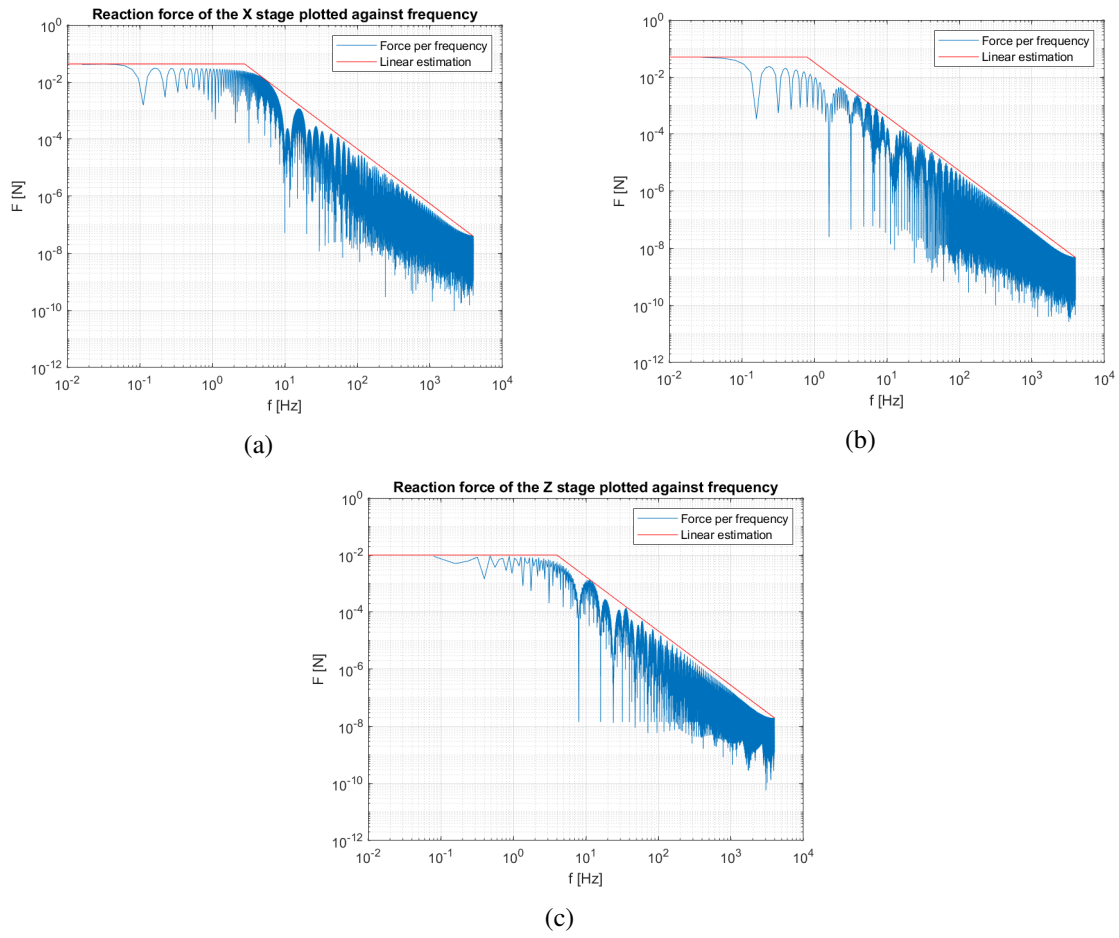


Figure 4.2: Reaction forces of the X stage, the vertical component of the Y stage and the Z stage plotted against frequency

4.4 Constraints in frequency domain

As later on in the project bode plots will be created for the X and Z direction of the table and with floor disturbances and reaction forces as inputs, it is desired to have a line in the bode plots, representing the maximum magnitude per frequency to stay within the constraints. As there will be two inputs, both the reaction forces and the floor disturbances, two different lines need to be made showing the maximum magnitude.

It is known what the maximum velocity can be at the test bench for both X and Y direction and the inputs are known as well. With the input and output of the system, the maximum magnitude can be determined, this is calculated in Equation 4.8. If this is done for all frequencies, it will give a line in the bode plot the model is not allowed to exceed.

$$mag(f) = \frac{out(f)}{in(f)} \quad (4.8)$$

Where mag is the magnitude, in and out are the in and outputs of the system, so as inputs there will be the reaction forces and the floor vibrations, as output, the velocity of the top of the test bench is obtained. All three variables are functions of frequency. This resulting graphs are shown below.

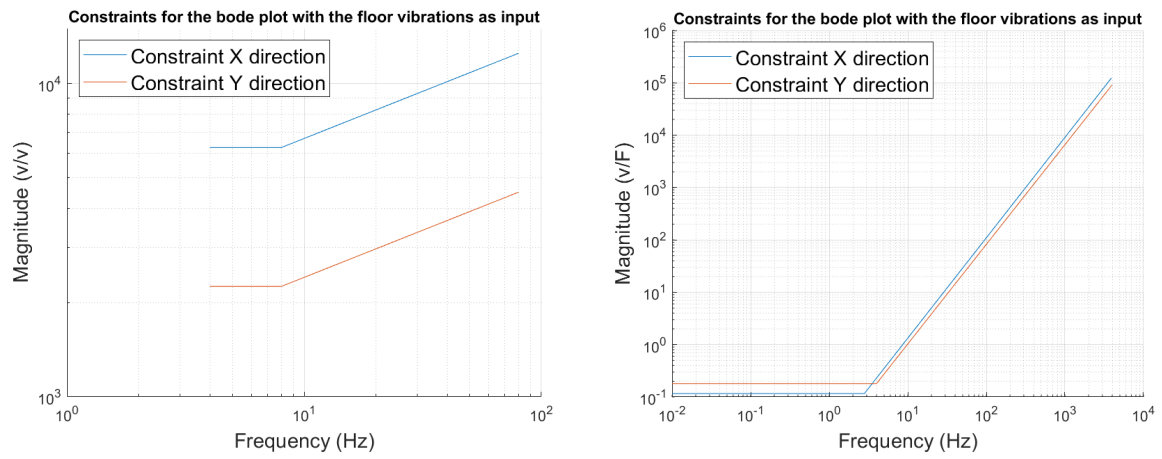


Figure 4.3: Constraints for the bode plots for floor vibrations and reaction force input

5 Analytical modelling

5.1 Assumptions

Before the analytical solution can be solved, some assumptions have to be made.

5.1.1 X direction

The top part is infinitely stiff

As the top part, see Figure 3.2b consists of the horizontal tabletop and the frame underneath it, all components are loaded in plane. The 4 vertical beams of the top part do not influence the stiffness as the top part is resting on the bottom part and friction force keeps it in place. Therefore, the vertical beams are not included in the force path. As all parts of the top part that are in the force path are loaded in plane, this entire part is assumed to be infinitely stiff.

The main beams and outer beams are clamped at the bottom

As can be seen in Figure 3.4a and Figure 3.3b, the main and outer beams are clamped at the bottom with an aluminum plate. As this plate has a significant thickness it can be assumed that there will be no significant bending in it. Thus, the main and outer beams are clamped at the bottom side.

The main beams will deform in an S-shape

The main beams are connected together at the top and bottom with horizontal beams as can be seen in Figure 3.3a. These horizontal beams prevent the main beams from having a free end as they force the top to remain horizontal. Therefore, an S-shaped bend in the main beams is expected.

All bolt connections are taken as infinitely stiff

For the analytical solution it is assumed that all bolt connections are infinitely stiff. This is done because the bolt connections are expected to be much stiffer compared with for example the bending of the aluminum beams.

5.1.2 Z direction

The main beam is infinitely stiff

The main beam is placed parallel with the outer beam, therefore the largest stiffness is dominant. The forces of the table go through the main beam in vertical direction, leading to a compressive stress in the beam. As metal beams are very stiff under tension or compression load, this stiffness will not influence the overall stiffness of the table compared to other, lower, stiffnesses. The stiffness of this beam is therefore assumed to be infinitely large.

The test bench is infinitely stiff

The test bench is assumed to be infinitely stiff in vertical direction. This is because it consists of two plates that are loaded in plane. A plate that is compressed in plane can still have buckling effects,

however, there are two steel tubes connecting the two plates together at different heights, reducing the free length of each plate, this is visible in Figure 3.5. The critical buckling force increases by $\frac{1}{L^2}$, reducing the free length of the plate with the tubes increases the required buckling load drastically. Therefore this stiffness will be set to be infinitely large.

Part of the connection between the bottom and top part is infinitely stiff

The top part rests at 8 points on the bottom part as was indicated in Figure 3.9b, the four points located on AD and BC are placed very close to the main beams. Because the distance between these point and the main beams is very small, there will be almost no bending moment in the green beam with the point loads on it due to the point loads from AD and BC. The other four point loads, located in the middle of this beam, do however create a significant bending moment. Therefore only these four points are taken into account for the stiffness determination.

All bolt connections are taken as infinitely stiff

For the analytical solution it is assumed that all bolt connections are infinitely stiff. This is done because the bolt connections are expected to be much stiffer compared with for example the bending of the aluminum beams.

5.2 Analytical approach

5.2.1 X direction

For the X direction, the weakest parts are expected to be the wheels and the main beams together with the outer beams. As all other beams are loaded in plane these are expected to not influence the stiffness of the system. As the wheels are rather complicated, these stiffnesses will only be determined by the measurements and not analytically.

Deflection beams

As described in section 5.1 the main beams are expected to deform in an S-shape. The connections on the top and bottom of the beam are assumed to be infinitely stiff. To calculate the S-shaped deformation of a beam, Equation 5.1 can be used. For the outer beams, a C-shaped deformation is assumed where the bottom side is clamped and the top side is free to move. The formula to calculate this deformation is given in Equation 5.2[1].

$$k = 12 \cdot \frac{E \cdot I}{l^3} \quad (5.1)$$

$$k = 3 \cdot \frac{E \cdot I}{l^3} \quad (5.2)$$

where c is the stiffness, E the Youngs' Modulus, I the area moment of inertia and l the length of the beam.

Table 5.1 shows the values inserted in the equations above and the resulting stiffnesses. The two beams are placed in parallel, therefore the individual stiffnesses can be added up. The resulting stiffness needs to be multiplied by four as there are four main beams and four outer beams, these beams are also placed

in parallel between themselves. The resulting values in Table 5.1 are already multiplied by four. The resulting overall stiffness after adding the two values is $1.04 \cdot 10^7$ [N/m].

Table 5.1: Caption

	Main beam	Outer beam	Unit
E	69	69	GPa
I	$57.3 \cdot 10^{-8}$	$19.6 \cdot 10^{-8}$	m^4
l	0.582	0.584	m
c	$9.63e6 \cdot 10^6$	$8.15e6 \cdot 10^5$	N/m

5.2.2 Z direction

For the Z direction of the test setup, the more compliant parts are the top part (the tabletop and the frame underneath it) and the wheels. As the wheels are rather complicated to determine analytically due to the ball bearings and this is out of the scope of this project, these stiffnesses will only be determined with measurements. The tabletop will be computed analytically before the measurements.

Stiffness of the top part

As the legs of the testbench are located right above the top beams, this is where the force will go through as it always takes the shortest path. Therefore the force will first have to go through the plane AEFD and after that, it can either go through AD into the top beam or via EF.

There are two stiffnesses present in the tabletop, first the stiffness of the two planes where the legs of the testbench are placed upon. Second, the bending stiffness of the top beam. These stiffnesses are placed in series.

Stiffness of the tabletop

On the table top, there is a bending of the plate expected creating a bowl like shape in the two rectangular spaces of the frame. The point loads are taken together right in the middle resulting in one point load for the formula for simplicity. The formula for this deformation is given below[4].

$$\Delta_{Tabletop} = \frac{\alpha * F * b^2}{E * t^3} \quad (5.3)$$

In this formula, F is the force due to the load, b is equal to the smaller side of the rectangle, E is the Youngs' Modulus and t is equal to the thickness of the material. The α value can be determined with the length ratio a/b, where a is the length of the longer side of the rectangle. The determination of the α value is shown in subsection B.1.1. The resulting deformation together with the used values is given in Table 5.2.

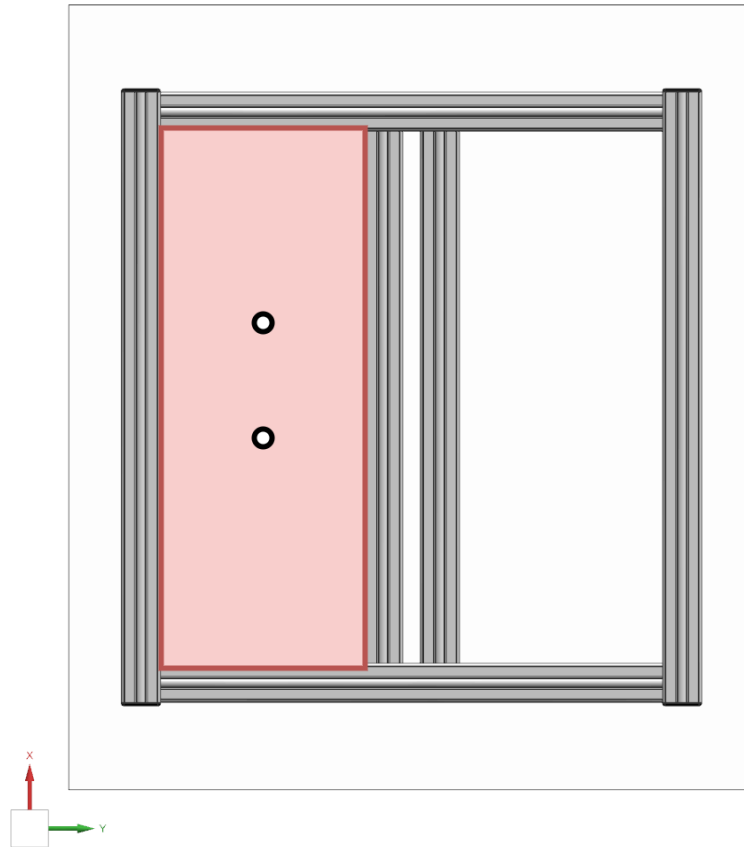


Figure 5.1: Deforming plane of the tabletop marked red with the point loads of the test bench marked.

Table 5.2: Deformation of the tabletop and the used values.

	tabletop	Unit
α	0.0805	[-]
F	135	N
b	0.2325	m
E	8	MPa
t	0.04	m
d	1.1	mm

With these deformations known, the stiffness of the tabletop can be computed. This is done by dividing the load by the deformation. It is multiplied by two as there are two planes next to each other and therefore they are in parallel.

$$k = \frac{2 \cdot F}{d} = 2.35 \cdot 10^5 [N/m] \quad (5.4)$$

Stiffness of the top beam

Because the two point loads are close together, they are taken as one point load in the middle of the top beam. A representation of this is given in Figure 5.2. The formula used is given below[1]. The stiffness can then be computed by dividing the load with the deformation and multiply it by two as there are two

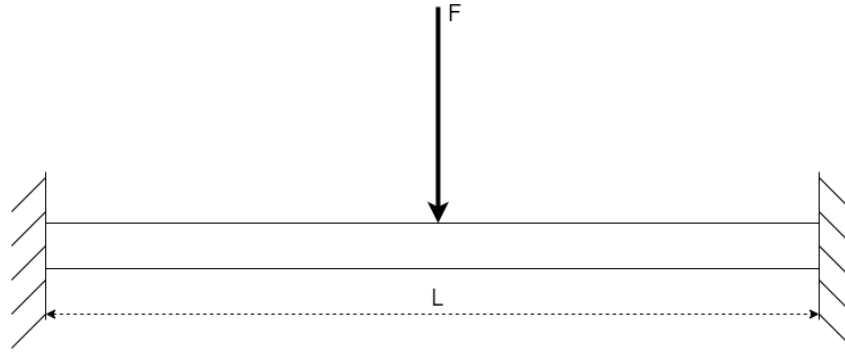


Figure 5.2: Representation of the load on the top beam

beams. The table with the used values and the resulting deformation and stiffness is given in Table B.2.

$$d = \frac{F \cdot L \cdot a^2}{6 \cdot E \cdot I} \cdot \left[3 \cdot \frac{b}{L^3} \cdot (L - z)^2 - \left(1 + \frac{2 \cdot b}{L} \right) \cdot \frac{(L - z)^3}{L^3} \right] \quad (5.5)$$

Where F is the applied force, L the length of the beam, a the distance at the left of the point force, b the distance at the right of the point force, E the Youngs' Modulus, I the area moment of inertia and z the distance where the deformation is measured.

Table 5.3: Stiffness of the top beam and the used values.

	Value	Unit
E	69	GPa
I	11.7	cm ⁴
L	0.61	m
a	0.305	m
b	0.305	m
z	0.305	m
k	1.37 · 10 ⁷	N/m

The resulting stiffness of the table top assembly is then equal to

$$k = \frac{1}{\frac{1}{k_{tabletop}} + \frac{1}{k_{topbeam}}} \quad (5.6)$$

The resulting stiffness for the table top assembly is equal to 2.30 · 10⁵ [N/m]

5.3 Lumped mass model

With the above determined stiffnesses and the masses of the test setup, a lumped mass model can be made. The corresponding bode plots will show the behaviour of the table for different frequencies. This behaviour can then be compared with the constraints in order to locate weaknesses in the design.

5.3.1 Masses

The total mass of the table setup needs to be split up in smaller masses which are being separated with springs. For the X direction, a split should be made at the axis of the wheel and at half the height of the main beams. For the Z direction, the split should be at the axis of the wheel as well and the other split

is through the middle of the horizontal frame of the top part. A clear representation of this is given in Figure 5.3. The corresponding masses are then m_A - m_C , the resulting values are shown in Table 5.4.

Table 5.4: Masses of the system

	Mass	Unit
m_A	23.6	kg
m_B	40.2	kg
m_C	37.6	kg

This gives the following masses that can be used for the transfer functions in the next section

Table 5.5: Masses used for the transfer functions.

	m1	m2
X direction	m_A	$m_B + m_C$
Z direction	$m_A + m_B$	m_C

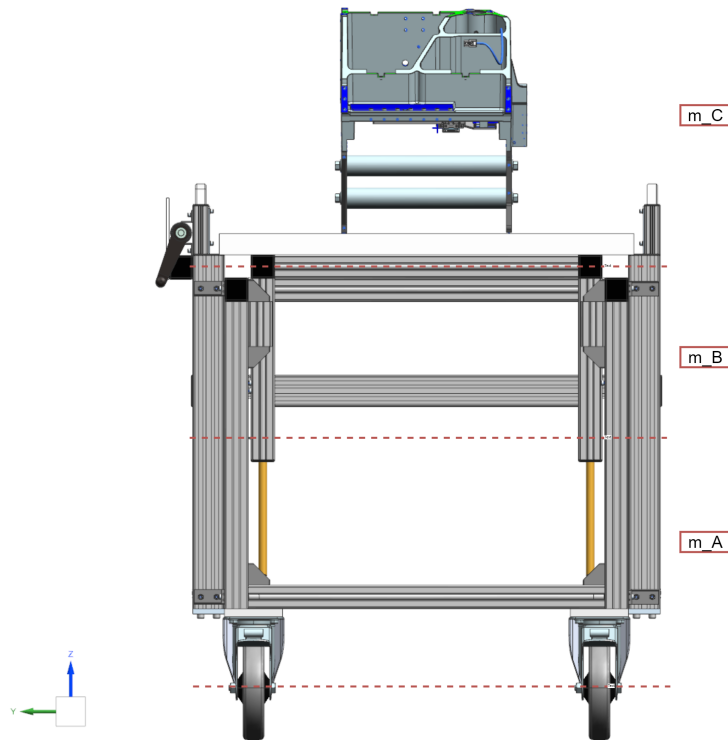


Figure 5.3: Division of the masses of the test setup.

5.3.2 Transfer functions

The representation of the lumped mass model is given in Figure 5.4a and Figure 5.4b for both the floor vibration as input as the reaction forces. With these lumped models, the transfer functions can be determined. These functions are given in Equation 5.7 and Equation 5.8. These transfer functions can then be plotted into bode plots once the stiffnesses of the wheels are known.



(a) Representation of the lumped mass model with the floor vibration as input. (b) Representation of the lumped mass model with the reaction force as input.

$$\frac{v_{out}}{v_{in}} = \frac{k_1 \cdot d_2 \cdot s^2 + (k_1 \cdot k_2) \cdot s}{m_1 \cdot m_2 \cdot s^5 + (m_1 \cdot d_2 + m_2 \cdot (d_1 + d_2)) \cdot s^4 + (m_1 \cdot k_2 + m_2 \cdot (k_1 + k_2) + d_1 \cdot d_2) \cdot s^3 + ((k_1 - k_2) \cdot d_2 + k_2 \cdot (d_1 + d_2)) \cdot s^2 + k_1 \cdot k_2} \quad (5.7)$$

$$\frac{v_{out}}{F_{in}} = \frac{m_1 \cdot s^3 + (d_1 + d_2) \cdot s^2 + (k_1 + k_2) \cdot s}{m_1 \cdot m_2 \cdot s^5 + (m_2 \cdot (d_1 + d_2) + m_1 \cdot d_2) \cdot s^4 + (m_2 \cdot (k_1 + k_2) + m_1 \cdot k_2 + d_1 \cdot d_2) \cdot s^3 + (d_2 \cdot k_1 + d_1 \cdot k_2) \cdot s^2 + k_1 \cdot k_2 \cdot s} \quad (5.8)$$

The above transfer functions have been validated with a Simscape model, the model used to verify the functions is shown in Figure A.5.

Damping

There is also some damping present, the damping ratio in metal structures is 0.02-0.04[2]. The value 0.02 is taken as this results in the highest peaks and therefore the worst case scenario. The damping coefficient which can be inserted in the transfer function is computed below.

$$d = 2 \cdot \zeta \cdot \sqrt{m \cdot k} \quad (5.9)$$

Where d is the damping coefficient, ζ the damping ratio, m the mass and k the stiffness. This damping coefficient can then be computed for every transfer function with the corresponding mass and stiffness.

6 Measurements

6.1 Instrument selection

The tools used for the measurements are **BBA 422 - 3 SM**, **Digital Indicator ID-C112XB** and **FH500**. The first one being a scale, the second one a digital indicator (DI) and the third one a force gauge (FG) to measure displacement. The total range and readability is shown in the table below.

	Range/capacity	Accuracy
Scale	60 [kg]	20 [g]
DI	12.7 [mm]	0.02 [mm]
FG	500 [N]	0.10 [N]

To verify that these tools have the suitable accuracy, the maximum measurable stiffness and the accuracy needs to be computed of the tools. The computation of the maximum measurable stiffness is given in the equation below.

$$k_{max} = \frac{F_{max}}{\Delta_{min}} \quad (6.1)$$

where k_{max} is the maximum stiffness, F_{max} is the maximum force and Δ_{min} is the smallest readable value on the DI.

In case the scale is used, the maximum force is $60[kg] \cdot 9.81[\frac{m}{s^2}]$. The minimum distance is 0.02mm. This results in the maximum measurable stiffness being $29.4 \cdot 10^6$ [N/m]. If the force gauge is used, the maximum force is 500N and the minimum distance again 0.02mm resulting in a maximum stiffness of $25.0 \cdot 10^6$ [N/m]

The error of the measurement can be computed with the accuracy of the tool itself. The error of the scale can be computed with the following equation, where e_m stands for the accuracy of the scale.

$$Error = \frac{e_m}{m_{max}} = \frac{0.02}{60} = 0.03\% \quad (6.2)$$

For the force gauge, the error is computed below

$$Error = \frac{e_m}{F_{max}} = \frac{0.10}{500} = 0.02\% \quad (6.3)$$

The error of the DI in Z direction can be obtained by first computing the expected displacement. This is equal to the force divided by the expected stiffness. The stiffness is equal to $7.51e4$ [N/m] and the total force is $60[kg]$ which is equal to 588.6 [N]. This gives an expected displacement of 3.6mm. The total accuracy of the DI is therefore equal to:

$$Error = \frac{e_{DI}}{\Delta_{expected}} = \frac{0.02}{3.6} = 0.56\% \quad (6.4)$$

6.2 Test plan

Before the measurements can be done, a test plan needs to be defined. The test plans for this project are given below

X direction

1. Screw the force gauge on the spindle and screw it in a horizontal orientation such that the force gauge is at the same height as the tabletop.
2. Tie a rope of around 7m length such that it loops around the tabletop and is connected to the force gauge.
3. Place the measurement tool on the desired location.
4. Read out the value on the measurement tool.
5. Turn the spindle around 180° and read out the value again.
6. Repeat the previous step until a force of around 50N is reached.
7. Repeat step 5-7 around 4 times.

Z direction

1. Find three masses of around 6-8kg.
2. Weigh the masses and calculate the force exerted by each mass.
3. Place the measuring tool at the desired location. This can be done by assembling a steel part to the frame of the table.
4. Mark the location where the test bench is supposed to stand to ensure it is placed on the same spot multiple times.
5. Read out the value on the measurement tool.
6. Place the testbench on the tabletop and read out the value of the measurement tool
7. Apply the additional weights one-by-one while reading out the value on the measurement tool
8. Repeat step 5-7 around 10 times.

6.3 Measurements

6.3.1 X direction

For the X direction, two different measurements were done. First, the force was applied at the tabletop and the DI was placed at the same height as the aluminum plate above the wheels, this measurement will give the stiffness of the four wheels at the bottom combined. Second, the wheels were removed and the frame was placed on the floor. The digital indicator was placed at the same height as the tabletop. This measurement will give the stiffness of the frame.

After having set up the DI at the correct spot, the tensile force at the force gauge was turned to around 12-16N as initial value to make sure there was tension on the rope. There were around 10 measurements done before the 50N mark was reached, therefore only four cycles were done as the amount of data points was quite large. The reason for the cap being at 50N is that the forces expected during the test are assumed to be quite small. A moving mass of 5kg with an acceleration of $1[m/s^2]$ are the typical forces expected during the tests, therefore, applying a large force might give false results if there are non linear stiffnesses in the system.

Some figures of the setup during testing are shown in section A.3 together with the obtained measurement results.

Table 6.1: Stiffnesses obtained during the measurement in X direction

	k	Unit
Wheels	$8.5 \cdot 10^4$	[N/m]
Frame	$3.8 \cdot 10^5$	[N/m]

6.3.2 Additional measurement

The measured stiffness of the frame is $3.8 \cdot 10^5$ [N/m], this is a factor of 27.5 lower than the analytically determined value. In order to find the source of this deviation, a second measurement has been done. This measurement excludes the table top assembly and only measures the stiffness of the table frame. If this measurement differs from the previous measurement, the conclusion can be drawn that the connection between the table top assembly and the frame assembly is not as stiff as expected. If the results are almost the same, the mistake is most likely made in the assumptions.

For this measurement the DI was placed against the top of the bottom part, thus excluding the top part and the connection between the top and bottom part. The resulting stiffness of this measurement was $5.9 \cdot 10^5$ [N/m]. This stiffness differs from the previously measured stiffness with a factor of around 1.6, concluding that there are indeed some imperfections in the table between the bottom part and the tabletop. This second measurement was still not close to the analytical stiffness. That would imply that there still one or more important stiffnesses in the frame still undetermined. It is however with this setup impossible to determine where these stiffnesses are located and how many there are.

6.3.3 Z direction

During the experiment, three different stiffnesses have been measured. First of all, the stiffness of the tabletop with respect to the frame underneath it. The other two stiffnesses are those of the two types of wheels, caster and fixed. Pictures of the setup can be found in section A.3.

The DI's have been set up at the corresponding locations and every measurement the 0kg value was read out, this is the displacement with no mass added on the table. This has been done every cycle as the initial value of the DI's could change due to external factors. After that, the frame was added on the table and the displacements were noted, next up, an additional mass was added on top of the frame another three times resulting in a total of 5 readings for each run. This process was repeated 15 times to get an accurate combined result.

In the experiment, the displacement has been measured under a specific load, the resulting displacements are visualized in section A.3. The mass indicated in the table is the total mass put on the table, this mass has to be divided by two for the tabletop and divided by four for the two wheels to have the exact mass on that specific component. This is allowed due to symmetry on the table and the load being applied to the center of the tabletop.

With the mass and therefore the force known and the displacements, the stiffnesses of the wheels and the tabletop can be computed. To get these stiffnesses the force exerted on the part needs to be divided by the displacement of that part. The resulting stiffnesses are listed below.

The stiffness of the table top that has been measured differs with a factor of 1.18. As the experimental and analytical stiffness are almost the same, the conclusion can be drawn that all expected stiffnesses have been accounted for at the table top assembly.

Table 6.2: Stiffnesses obtained during the measurement in Z direction

	K	Unit
Table top	1.95e5	N/m
Fixed wheel	3.00e5	N/m
Caster wheel	1.48e5	N/m

6.4 Analysis

6.4.1 X direction

As the measurements turned out to be not supporting the analytical solution. The resulting bode plot will not be representative. It was assumed that the important stiffnesses would mainly be in the wheels and in the bending of the vertical beams of the frame. This turned out to not be the case, the bode plots will still be made and shown, indicating what it would have looked like. Note that these plots can not be used for further research.

For the resulting bode plot, the stiffnesses of the first measurement have been used with the same masses as with the analytical solution. Included in the bode plot is the constraint which was defined in section 4.4. If the bode plot stays underneath this line, its magnitude is not big enough to create significant disturbances to make the tests fail. If it does pass this line, some changes need to be made to the setup to correct for that. The resulting bode plots are given in Figure 6.3 and Figure 6.4.

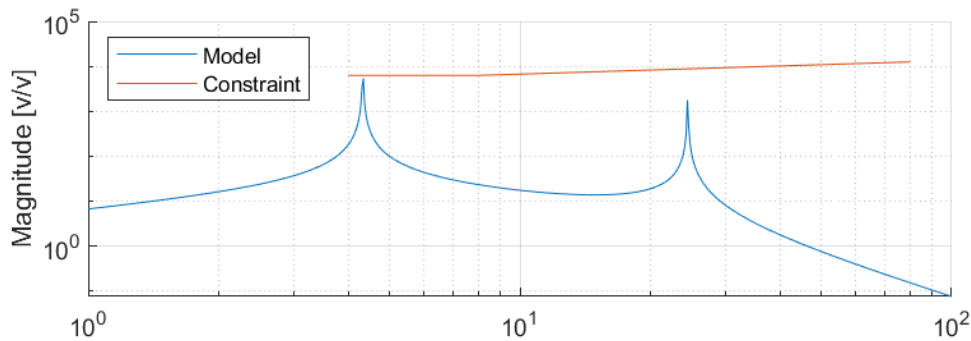


Figure 6.1: Bode plot of the X direction with floorvibrations as input

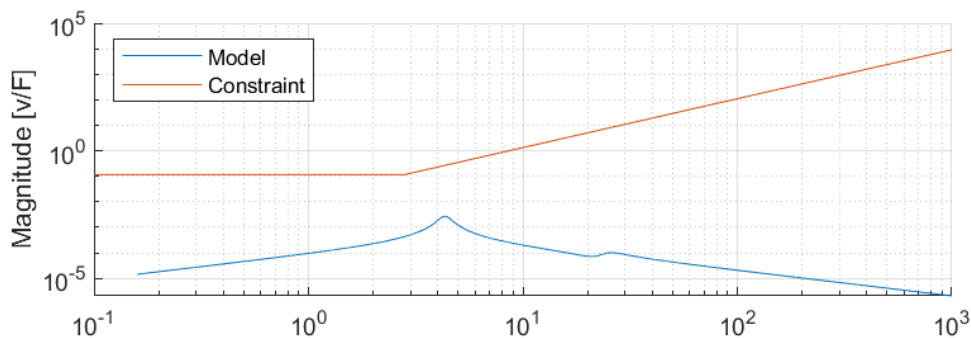


Figure 6.2: Bode plot of the X direction with reaction force as input

It can clearly be seen that the model does not exceed the constraint line at any frequency. This backs up the idea that not all important stiffnesses are taken into account as the production tests show poor results for the X direction.

6.4.2 Z direction

The obtained stiffnesses of the measurements have been implemented in the transfer functions created in Figure 6.3 and Figure 6.4. The resulting bode plots are shown below. It can be seen that the model does exceed the constraint line, it would be expected that the model will exceed the constraint line at some points. Therefore the question needs to be asked whether the model is correct and if there are more stiffnesses that need to be taken into account.

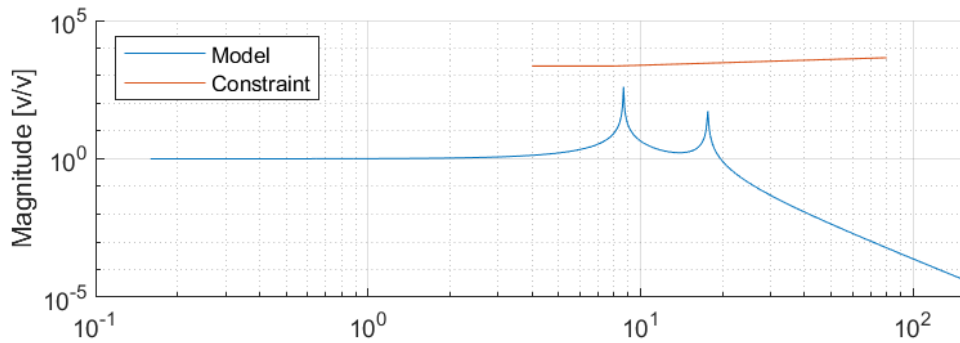


Figure 6.3: Bode plot of the Z direction with floorvibrations as input

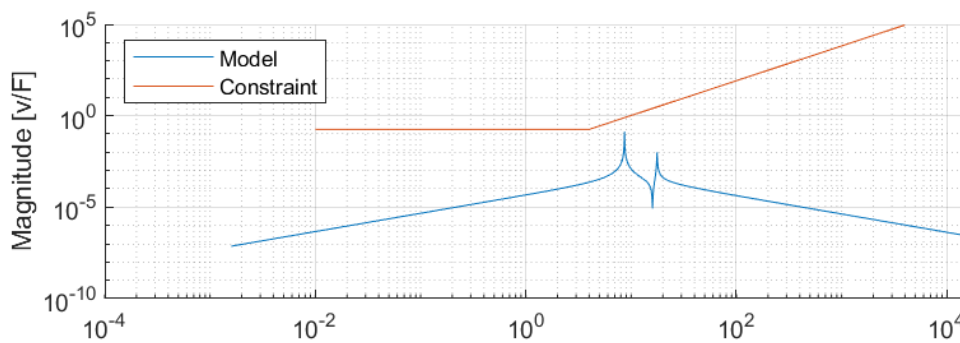


Figure 6.4: Bode plot of the Z direction with reaction force as input

7 Conclusion

The goal of this report is to analyze the behaviour of the assembly table when external disturbances, through the floor and due to reaction forces, are applied. This was done by first setting up the correct requirements of the system for different frequencies. Transfer functions have been created with disturbances from the floor and disturbances due to reaction forces of the stage itself as inputs and disturbance velocities as outputs. The stiffnesses of the assembly table have been found with measurements and have been validated with an analytical solution. These transfer functions were then plotted into bode plots. These plots can then be compared to the defined requirements and analyzed.

The found values of the stiffness for the table top assembly with the analytical approach and the measurements differs with a factor of 1.18. The found stiffness of the X direction differs with a factor of 27.5. This stiffness is therefore not as expected and needs to be reconsidered.

The bode plots for both X and Z direction were both complying with the constraints, as this is not the expected outcome, both directions still need further investigation. For the X direction the recommendation is done to do dynamic testing instead of static testing. As the measurements showed, the table behaves not as expected and the source of this compliance is unknown. For the Z direction a static test, measuring the displacement of the table top assembly with respect to the fixed world is recommended to verify all compliant stiffnesses are accounted for.

8 Recommendations

During this project several topics came up that would require more research. There have also been some design flaws found with the current setup.

8.1 Recommendations for future research

A static test should be performed for the Z direction. During this project, the individual stiffnesses of the wheels and the tabletop have been determined. The assumption has been made that these are the only important stiffnesses, it can however not be said with certainty without proving it. Therefore, doing a static test on the bottom of the tabletop with the digital indicator anchored to the fixed world would give the total stiffness of the setup. If the stiffness of the wheels and the top part coincide with this stiffness, the conclusion can be made that these are indeed the only important stiffnesses.

A dynamic test is suggested for the table as, especially in X direction, quite some stiffnesses are yet unknown. With dynamic testing, an FRF of the entire table can be made and with proper placement of the sensors, FRFs of specific parts can be made. The peaks in the FRF of the entire setup and the FRF of the specific parts will have some overlapping peaks, from there can be concluded which specific parts are problematic.

The floor vibrations are given as velocities as function of frequency. As the direction is not defined in the case description, this can be looked into. Currently it is assumed that the velocity is the same for all three dimensions. In practice, this might not be the case. To verify this, some vibration measurements can be done on the production floor giving more precise values for the floor vibrations.

8.2 Findings on the current setup

The outer beam is slightly too long on the tables, the top of the beam is therefore slightly higher than the frame. This results in the tabletop resting on the four outer beams instead of the frame of the table. This is a design flaw as the outer beams are placed closely together at the sides of the table resulting in the table becoming a seesaw.

The wheels have a lot of play in the direction perpendicular to the driving direction. Therefore in X direction, the entire table is shaking as it is feeling the play of the wheels instead of the stiffness of the wheels

A Appendix A

A.1 Constraints

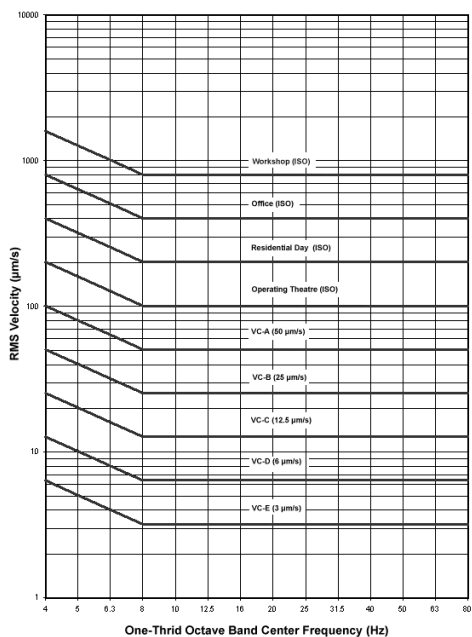


Figure A.1: Graph showing the amplitude of the floor vibration as a function of frequency

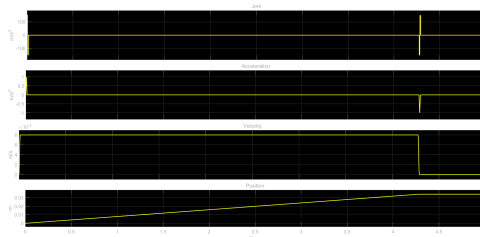


Figure A.2: Motion profile of the X direction

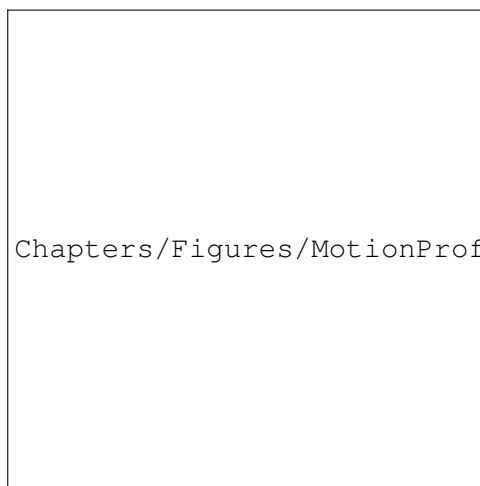


Figure A.3: Motion profile of the Y direction

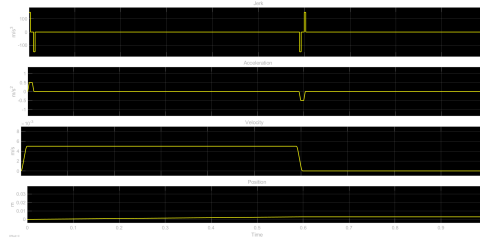


Figure A.4: Motion profile of the Z direction

A.2 Analytical approach

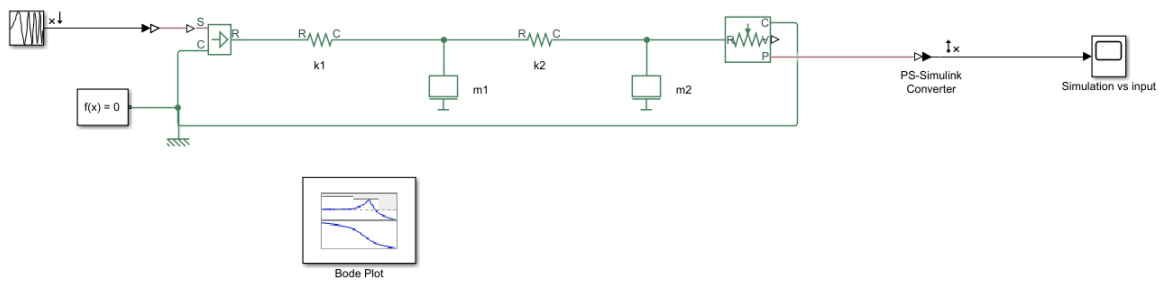


Figure A.5: Simscape model used to verify the transfer functions

A.3 Measurements

Figures of the test setup in X direction



Figure A.6: Overview of the test setup.



Figure A.7: Overview of the test setup.



Figure A.8: Placement of the DI for the measurement of the wheel stiffness.



Figure A.9: Spindle used to hold the force gauge and apply tension on the wire



Figure A.10: The wire being routed around the table and being kept from sliding down

Figures of the test setup in Z direction

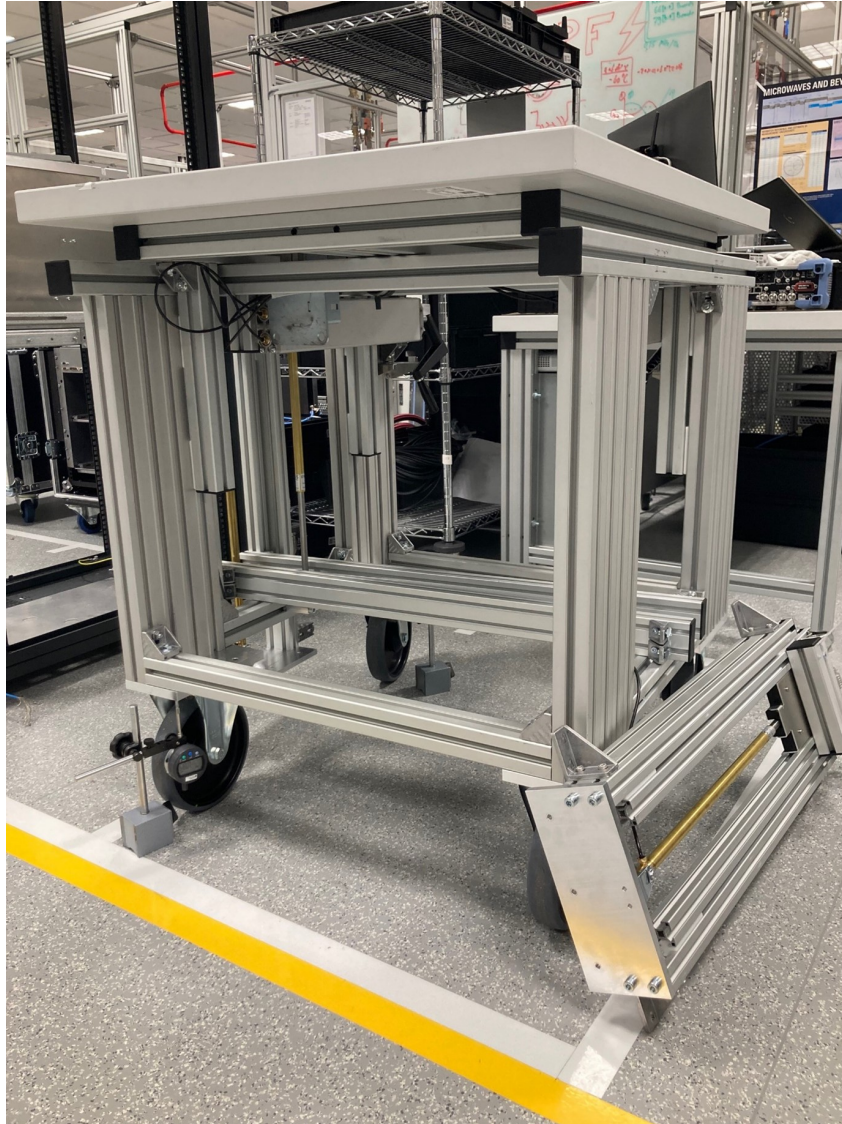


Figure A.11: Overview of the test setup.



Figure A.12: Placement of the DI underneath the tabletop.

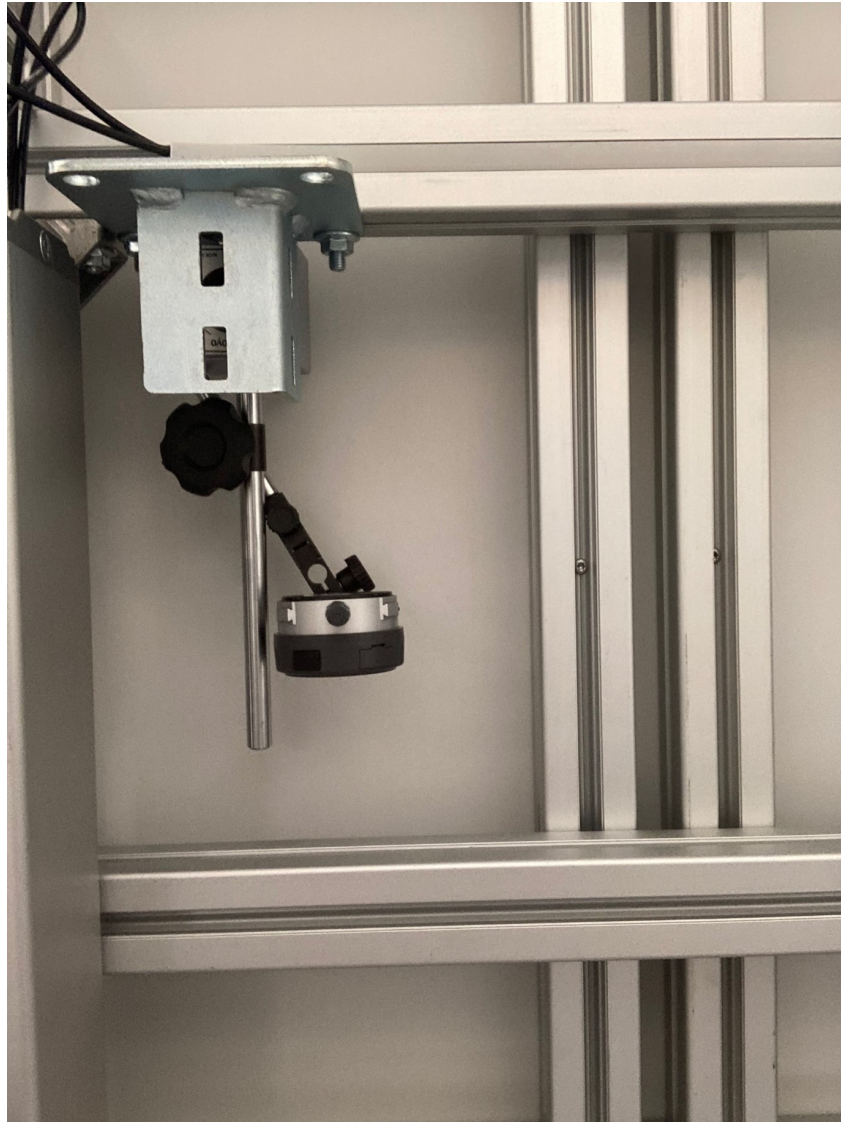


Figure A.13: Placement of the DI underneath the tabletop.



Figure A.14: Placement of the DI at the wheels.

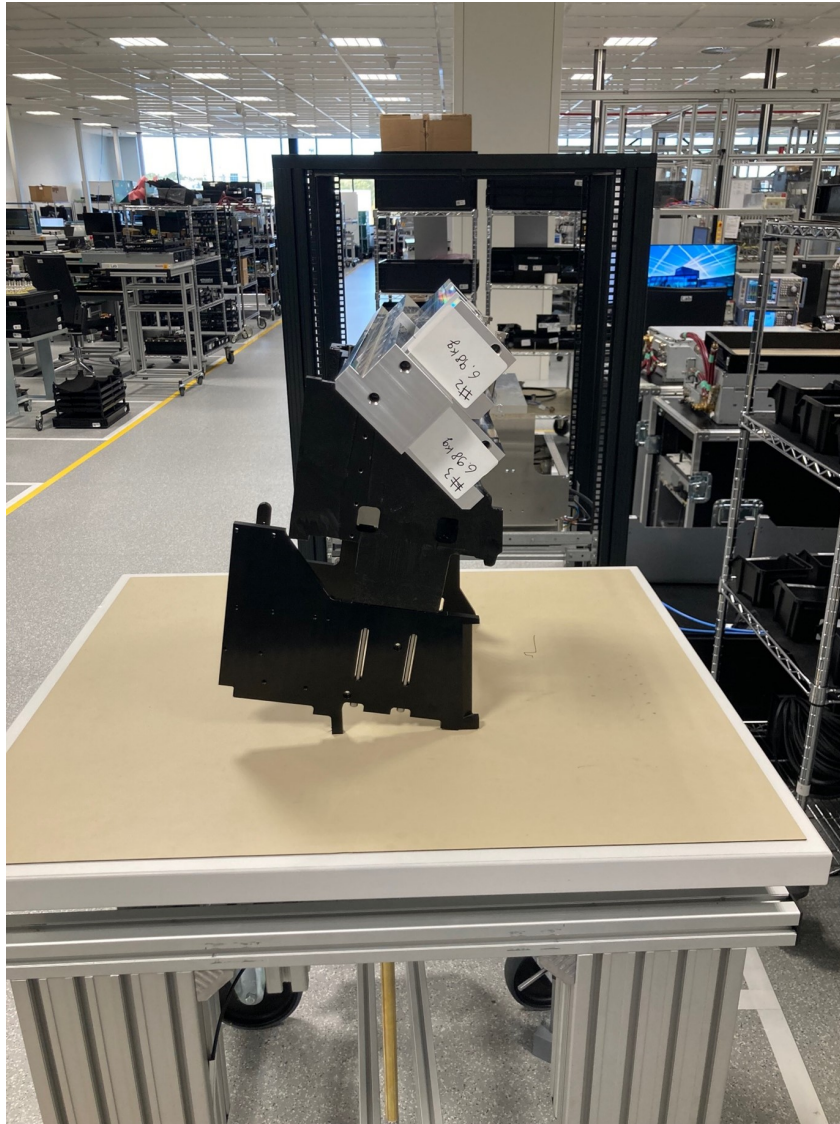


Figure A.15: The mass put on top of the testbench

Test results of the X direction

Table A.1: Measurement of the frame without the wheels with the rope attached to the tabletop, values are in mm.

Measurement 1		Measurement 2		Measurement 3		Measurement 4	
F [N]	d [mm]	F [N]	d [mm]	F [N]	d [mm]	F [N]	d [mm]
14.7	1.481	33.0	1.540	19.0	1.512	14.8	1.505
20.6	1.495	37.6	1.553	24.7	1.525	18.7	1.513
24.8	1.501	41.4	1.564	30.1	1.537	22.6	1.522
29.3	1.513	44.4	1.574	34.8	1.550	25.6	1.530
33.4	1.524	48.7	1.585	39.3	1.563	29.5	1.540
37.1	1.535	52.7	1.599	43.1	1.574	32.8	1.547
40.5	1.546			47.7	1.584	36.5	1.557
44.2	1.557			52.1	1.598	40.0	1.576
47.7	1.571						
50.2	1.583						

Table A.2: Measurement of the frame without the wheels with the rope attached to the top of the bottom part, values are in mm.

Measurement 1		Measurement 2		Measurement 3		Measurement 4	
F [N]	d [mm]	F [N]	d [mm]	F [N]	d [mm]	F [N]	d [mm]
9.4	2.748	21.0	2.765	20.1	2.767	20.5	2.768
11.5	2.749	26.5	2.776	25.1	2.775	26.3	2.779
13.0	2.753	31.9	2.785	29.7	2.783	30.9	2.787
15.0	2.755	36.0	2.791	33.7	2.789	35.7	2.795
17.0	2.760	40.0	2.799	37.8	2.797	39.8	2.801
19.3	2.763	43.5	2.804	41.5	2.803	44.3	2.809
21.8	2.768	46.4	2.810	45.4	2.810	47.4	2.811
23.9	2.771						
26.2	2.776						
28.6	2.779						
31.4	2.784						
34.1	2.787						
37.0	2.792						
39.7	2.797						
42.2	2.803						
44.8	2.806						

Table A.3: Measurement of the stiffness of the wheels, values are in mm.

Measurement 1		Measurement 2		Measurement 3	
F [N]	d [mm]	F [N]	d [mm]	F [N]	d [mm]
12.4	2.065	16.0	3.665	12.1	3.859
16.9	2.124	19.6	3.726	14.8	3.891
22.1	2.175	22.7	3.771	17.5	3.920
25.7	2.212	25.7	3.813	23.5	3.990
31.1	2.261	28.8	3.856	26.6	4.028
34.9	2.298	31.3	3.891	29.3	4.058
38.4	2.330	34.4	3.925	31.5	4.083
		36.9	3.955	33.9	4.108
		39.1	3.986		
		42.1	4.024		
		45.2	4.060		

Test results of the Z direction

Table A.4: Displacements of the tabletop, values are in [mm]

#	0kg	19.35kg	26.51kg	33.49kg	40.47kg
1	0.803	0.852	0.869	0.887	0.908
2	0.804	0.851	0.870	0.893	0.907
3	0.800	0.850	0.867	0.887	0.907
4	0.800	0.855	0.867	0.883	0.907
5	0.800	0.853	0.868	0.888	0.908
6	0.802	0.853	0.870	0.890	0.909
7	0.800	0.856	0.871	0.889	0.908
8	0.802	0.854	0.866	0.885	0.905
9	0.800	0.855	0.868	0.887	0.909
10	0.803	0.858	0.872	0.887	0.908
11	0.802	0.855	0.868	0.885	0.906
12	0.801	0.858	0.868	0.885	0.906
13	0.803	0.859	0.870	0.886	0.907
14	0.804	0.852	0.870	0.892	0.907
15	0.804	0.851	0.869	0.886	0.906

Table A.5: Displacements of the fixed wheel, values are in [mm]

#	0 kg	19.35kg	26.51kg	33.49kg	40.47kg
1	7.057	7.083	7.088	7.094	7.101
2	7.064	7.096	7.102	7.107	7.112
3	7.077	7.101	7.105	7.109	7.112
4	7.078	7.101	7.106	7.115	7.117
5	7.082	7.099	7.106	7.112	7.115
6	7.083	7.103	7.111	7.117	7.120
7	7.084	7.103	7.110	7.117	7.119
8	7.085	7.103	7.109	7.117	7.122
9	7.085	7.108	7.114	7.121	7.120
10	7.087	7.107	7.111	7.117	7.122
11	7.083	7.103	7.110	7.117	7.123
12	7.088	7.107	7.112	7.120	7.123
13	7.087	7.108	7.114	7.122	7.124
14	7.091	7.105	7.111	7.117	7.120
15	7.091	7.111	7.116	7.122	7.124

Table A.6: Displacements of the caster wheel, values are in [mm]

#	0 kg	19.35kg	26.51kg	33.49kg	40.47kg
1	5.928	5.955	5.969	5.979	5.996
2	5.931	5.960	5.975	5.990	6.003
3	5.933	5.959	5.974	5.986	5.998
4	5.935	5.961	5.974	5.983	5.996
5	5.937	5.960	5.974	5.987	6.003
6	5.939	5.962	5.974	5.986	5.998
7	5.939	5.962	5.973	5.983	5.999
8	5.936	5.962	5.975	5.987	6.001
9	5.937	5.964	5.977	5.988	6.000
10	5.941	5.962	5.976	5.986	5.999
11	5.933	5.959	5.974	5.982	5.994
12	5.934	5.960	5.973	5.984	5.997
13	5.935	5.964	5.977	5.987	6.000
14	5.939	5.969	5.982	5.994	6.008
15	5.942	5.966	5.978	5.989	6.004

B Appendix B

B.1 Analytical solution

B.1.1 α Values

The *alpha* value can be determined with the a/b ratio of the plane. The table below was provided with the equation. The a/b ratio for the tabletop is equal to 2.62[-], because this value is not exactly given in the table, a polynomial has been made of the points in the table with the least-squares method. The resulting graph can be seen in Figure B.1. The α value that corresponds with the a/b ratio is equal to 0.0805.

Table B.1: The a/b ratios with the corresponding α values.

a/b	1.0	1.2	1.4	1.6	1.8	2.0	∞
α	0.0611	0.0706	0.0754	0.0777	0.0786	0.0788	0.0791

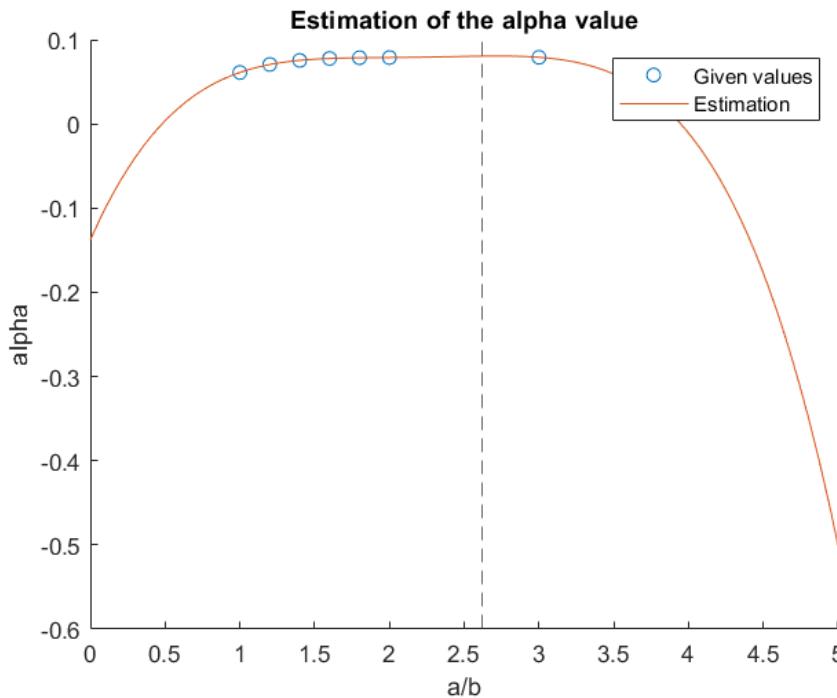


Figure B.1: Estimation of the alpha values

B.1.2 Derivation of the transfer function with floor disturbance as input

For both masses, the force balance equations can be set up. The equation of mass one is given in Equation B.1 and for mass two it is given in Equation B.2. These equations can be converted to the frequency domain by applying the Laplace transform, the resulting equations are given in Equation B.3 and Equation B.4 for mass one and two respectively.

$$m_1 \cdot \ddot{u}_1 = k_1 \cdot (x - u_1) + k_2 \cdot (u_2 - u_1) + d_1 \cdot (\dot{x} - \dot{u}_1) + d_2 \cdot (\dot{u}_2 - \dot{u}_1) \quad (\text{B.1})$$

$$m_2 \cdot \ddot{u}_2 = k_2 v(u_1 - u_2) + d_2 \cdot (u_1 - u_2) \quad (\text{B.2})$$

$$m_1 \cdot s^2 \cdot U_1 = k_1 \cdot X - (k_1 + k_2 + (d_1 + d_2) \cdot s) \cdot U_1 + (k_2 + d_2 \cdot s) \cdot U_2 \quad (\text{B.3})$$

$$m_2 \cdot s^2 \cdot U_2 = (k_2 + d_2 \cdot s) \cdot U_1 - (k_2 + d_2 \cdot s) \cdot U_2 \quad (\text{B.4})$$

The two equations in frequency domain can be combined into one equation by substituting them for U_1 . By substituting with U_1 , the equation has only U_2 and X as variables, this is the desired outcome as these are the input and output points of the system. After substitution the equation can be written in the form $\frac{U_2}{X}$. Finally as the input and output of the system are both in velocity, the entire equation needs to be multiplied with $\frac{s}{s}$ to go from U_2 and X to \dot{U}_2 and \dot{X}

B.1.3 Derivation of the transfer function with reaction forces as input

B.1.4 Deformation top beams

Because the two point loads are close together, they are taken as one point load in the middle of the top beam. The formula used is given below. The stiffness can then be computed by dividing the load with the deformation and multiply it by two as there are two beams. The table with the used values and the resulting deformation and stiffness is given in Table B.2.

$$d = \frac{F \cdot L \cdot a^2}{6 \cdot E \cdot I} \cdot \left[3 \cdot \frac{b}{L^3} \cdot (L - z)^2 - \left(1 + \frac{2 \cdot b}{L} \right) \cdot \frac{(L - z)^3}{L^3} \right] \quad (\text{B.5})$$

Where F is the applied force, L the length of the beam, a the distance at the left of the point force, b the distance at the right of the point force, E the Youngs' Modulus, I the area moment of inertia and z the distance where the deformation is measured.

Table B.2: Stiffness of the top beam and the used values.

	Value	Unit
E	69	GPa
I	11.7	cm^4
L	0.61	m
a	0.305	m
b	0.305	m
z	0.305	m
k	$1.37 \cdot 10^7$	N/m

B.2 Measurements

To be certain that the measurements were executed on a consistent way the standard deviation can be computed. This shows the spread between the measured values. Below is explained how this is done and the results are shown.

First of all the average value needs to be computed for the displacement. This is done by summing all the measurements and dividing by the amount of measurements done. With this average value the standard deviation of this measurement can be computed. The formula below has been used to compute this. The resulting values are stored in the tables below, together with the minimum and maximum value that were measured.

$$s = \sqrt{\frac{(\sum d - d_{avg})^2}{nr_{measurements}}} \quad (\text{B.6})$$

where d represents the displacement, d_{avg} the average displacement and $n_{measurements}$ the amount of measurements and Z is a constant value corresponding to a 90% confidence interval.

As the force values were not constant throughout the measurement, the distances have been divided by the applied forces, resulting in the distance per Newton being used for the computation of the values below.

Table B.3: Average value, standard deviation, minimum and maximum value of the measurements in X direction, the values are in μm

	average	s	min	max
wheels	11.97	1.92	9.07	16.9
frame first	2.88	0.80	1.43	5.43
frame second	1.66	0.47	0.48	2.67

Table B.4: Average value, standard deviation, minimum and maximum value of the measurements in Z direction, the values are in μm

	average	s	min	max
tabletop	5.14	0.84	2.87	6.88
Caster wheel	6.77	1.30	4.30	9.74
Fixed wheel	3.33	1.23	0.001	6.55

Bibliography

- [1] JPE innovations. Beam theory: Bending. <https://www.jpe-innovations.com/precision-point/beam-theory-bending/>, 2020.
- [2] JPE innovations. Structural damping properties of mechanical systems. <https://www.jpe-innovations.com/precision-point/structural-damping-properties-mechanical-systems/>, 2020.
- [3] JPE innovations. Third order point-to-point motion profile. <https://www.jpe-innovations.com/precision-point/third-order-point-to-point-motion-profile/>, 2022.
- [4] Warren C Young, Richard G Budynas, and Ali M Sadegh. *Roark's formulas for stress and strain (p.508-509)*. McGraw-Hill Education, 2012.